Arabian Journal of Chemistry (2015) xxx, xxx–xxx

King Saud University

Arabian Journal of Chemistry

www.ksu.edu.sa
www.sciencedirect.com

ORIGINAL ARTICLE

# Stigmasterol extracted from *Ficus hispida* leaves as a green inhibitor for the mild steel corrosion in 1 M HCl solution

**P. Muthukrishnan [a,*], P. Prakash [b,*], B. Jeyaprabha [c], K. Shankar [a]**

[a] *Department of Chemistry, Faculty of Engineering, Karpagam Academy of Higher Education, Coimbatore 641 021, India*
[b] *PG & Research Department of Chemistry, Thiagarajar College, Madurai 625009, India*
[c] *Department of Civil Engineering, Fatima Michael College of Engineering & Technology, Madurai 625020, India*

Received 9 April 2015; accepted 11 September 2015

**KEYWORDS**

Acid corrosion;
Mild steel;
Polarization;
SEM;
Adsorption

**Abstract** The anticorrosive potential of *Ficus hispida* leaf extract (FHLE) as a corrosion inhibitor in 1 M HCl was investigated using weight loss measurement as well as potentiodynamic polarization and electrochemical impedance spectroscopy (EIS) techniques. Stigmasterol as the major constituent of *F. hispida* was confirmed by Gas Chromatography–Mass Spectrometry (GC–MS). Inhibition efficiency of 90% was achieved with 250 ppm of FHLE at 308 K. Temperature studies revealed an increase in inhibition efficiency with decrease in temperature and activation energies increased in the presence of the extract. Cathodic and anodic polarization curves revealed that FHLE acts as mixed type inhibitor, but cathodic effect was more pronounced. Impedance diagrams showed that increasing FHLE concentration, increased charge transfer resistance and decreased double layer capacitance. The adsorption of FHLE on mild steel surface obeyed Langmuir adsorption isotherm. The morphology of the surface was examined by scanning electron microscopy (SEM) and the surface composition was evaluated using energy-dispersive X-ray (EDX) spectroscopy to verify the presence of inhibitor on the mild steel surface. The adsorbed film on the mild steel surface containing the FHLE inhibitor was also characterized by diffuse reflectance Fourier transform infrared spectroscopy (DRFT-IR) and X-ray diffraction (XRD) studies.


* Corresponding authors at: Faculty of Engineering, Department of Chemistry, Karpagam Academy of Higher Education, Coimbatore 641 021, Tamil Nadu, India. Tel.: +91 9994440669; fax: +91 4222980022 (P. Muthukrishnan). PG & Research Department of Chemistry, Thiagarajar College, Madurai 625009, Tamil Nadu, India. Tel.: +91 9842993931; fax: +91 4522312375 (P. Prakash).
E-mail addresses: muthukrish.karpagam@gmail.com (P. Muthukrishnan), kmpprakash@gmail.com (P. Prakash).
Peer review under responsibility of King Saud University.

Production and hosting by Elsevier

http://dx.doi.org/10.1016/j.arabjc.2015.09.005
1878-5352 

Please cite this article in press as: Muthukrishnan, P. et al., Stigmasterol extracted from *Ficus hispida* leaves as a green inhibitor for the mild steel corrosion in 1 M HCl solution. Arabian Journal of Chemistry (2015), http://dx.doi.org/10.1016/j.arabjc.2015.09.005

## 1. Introduction

Various methods are used to reduce corrosion rate of metal and alloys, among which the use of corrosion inhibitor is widely known. They reduce the corrosion rate mainly by increasing or decreasing the anodic and/or cathodic reactions and decreasing diffusion rate for reactants to the surface of the metal and the electrical resistance of the metal surface (Kamal and Sethuraman, 2012). During past decades, some commercial inhibitors have been synthesized and used successfully to inhibit corrosion of steel in acidic media (Soltani et al., 2010; Solmaza et al., 2011; Issaadi et al., 2011; Naderi et al., 2009; Muthukrishnan et al., 2014a). Nevertheless, most of these inhibitors are not eco-friendly but toxic and expensive. Therefore, the study of new non-toxic or environmentally safe corrosion inhibitors is essential to overcome this problem. The research in the field of eco-friendly corrosion inhibitors has been addressed toward the goal of using cheap, effective compounds at low or zero environmental impact. For industrial and large scale use, cost of the inhibitor, its toxicity, availability and environmental friendliness are very important. Several considerations have to be taken into account when choosing an inhibitor: Toxicity of the inhibitor can cause jeopardizing effects on human beings and other living species, cost of the inhibitor can be sometimes very high when the material involved is expensive or when the amount needed is huge, availability of the inhibitor will determine its selection and if the availability is low, the inhibitor becomes often expensive and environmental friendliness. Therefore apart from various organic inhibitors, the use of natural products which are eco-friendly and harmless has become popular (Muthukrishnan et al., 2013a,b,c, 2014b,c,d). Currently, researchers are being focusing on producing and testing eco-friendly corrosion inhibitors (Khaled, 2003), such as *Ananas sativum*, olive, lupine, fruit peel, Occimum viridis and Nypa fruticans Wurmb (Ating et al., 2010; El-Etre, 2007; Abdel Gaber et al., 2009; Cardozo Da Rocha et al., 2010; Oguize, 2006; Orubite and Oforka, 2004). *Ficus hispida* (Family; Moraceae) is an important woody, medicinal plant. It is commonly known as 'devil fig' and has a predominant place in Ayurveda, Siddha, Unani systems of medicine. The leaves and bark are purgative, antipyretic and are used in cardioprotective (Shanmugarajan et al., 2008a) antidiarrhoeal (Subhash et al., 2002) and antidiabetic activity (Ghosh et al., 2004). Earlier reports reveal that *F. hispida* leaves contain active phytochemical constituents such as oleanolic acid, bergapten, β-amyrin, β- sitosterol, hispidine and phenanthroindolizidine alkaloids (Shanmugarajan et al., 2008b; Peraza-Sanchez et al., 2002). The objective of the present work was to study the inhibitive action of FHLE on corrosion behavior of mild steel in 1 M HCl solution. Confirmation of FHLE corrosive inhibition was done through weight loss, AC impedance method, potentiodynamic polarization, SEM and EDX analysis, DRFT-IR and XRD. Additionally, thermodynamic and kinetic data were evaluated.

## 2. Experimental

### 2.1. Materials preparation

Composition of mild steel was C-0.05%, Mn-0.6%, P-0.36%, Si-0.03% and balance Fe. The steel specimens were mechanically cut into size of 2.5 × 2.5 × 0.4 cm for gravimetric measurements. Mild steel cylindrical rods of the same composition embedded in araldite with exposed area of 0.5 $cm^2$ were used for potentiodynamic polarization and electrochemical impedance measurements. The electrode was weld from one side to a copper wire used for electric connection. Before measurements, the specimens were mechanically polished with fine grade emery paper (4/0 grades), degreased in acetone, dried and stored in a dessicator. The solutions (1 M HCl) were prepared by dilution of an analytical reagent grade 33% HCl with triple-distilled water.

### 2.2. Extraction of F. Hispida Leaf Extract (FHLE)

*F. hispida* leaves were collected in Sirumalai Hills, Dindigul District, India. They were cut into small pieces, dried under shade conditions for 30 days and ground well into fine powder. 20 g of dried and powdered leaves of *F. hispida* was extracted with absolute ethanol in Soxhlet apparatus for 12 h. After completion of extraction, the extract was filtered and heated on a water bath at 60 °C until most of the ethanol evaporated. 0.8 g of the ethanol extract was digested in 1 l of 1 M HCl solutions (for weight loss and electrochemical measurements, respectively). From the stock solution (0.8 g/l), plant extracts test solutions were prepared at concentrations of 50, 100, 150, 200 and 250 mg/L.

### 2.3. Gas Chromatography–Mass Spectrometry (GC–MS) analysis

About 2 µl of the plant extract sonicated with n-hexane was analyzed by GC–MS (GC Clarus 500 Perkin Elmer model) equipped with mass detector (Turbo mass gold-Perkin Elmer) and column of 30 × 0.25 mm × 0.25 µm DF (Elite 5-MS). The oven was held at a temperature of 110 °C and programmed at 10 °C/min to 250 °C. Other operating conditions were as follows: carrier gas – He (99.99%), injector temperature – 250 °C and detector temperature – 280 °C. The identification of the essential components was performed using National Institute Standard and Technology Ver.2.1 library.

### 2.4. Gravimetric (weight loss) method

Weight loss measurements were performed as per ASTM method described previously (ASTM G, 1990 and Quraishi et al., 1997). In the gravimetric experiments, a previously weighted mild steel specimen was completely immersed in 100 ml of 1 M hydrochloric acid solutions without and with different concentrations of inhibitors. The beaker was inserted into a water bath maintained in the range 308–328 K for 2 h. After 2 h of immersion, the specimens were taken out from solution, washed with double distilled water, dried thoroughly and weighed. The weight of mild steel specimens before and after immersion was determined using an analytical balance with a precision of 0.1 mg. The experiments were done in triplicate and the weight losses were averaged. The weight loss ($W$) was used to calculate the corrosion rate (CR) and the inhibition efficiency (% IE) using the following relationship:

$$\mathrm{CR(mpy)} = \frac{534 \times W}{DST} \quad (1)$$

Please cite this article in press as: Muthukrishnan, P. et al., Stigmasterol extracted from *Ficus hispida* leaves as a green inhibitor for the mild steel corrosion in 1 M HCl solution. Arabian Journal of Chemistry (2015), http://dx.doi.org/10.1016/j.arabjc.2015.09.005

$$\%IE = \frac{(W_0 - W_i)}{W_0} \times 100 \quad (2)$$

Here $W = (W_b - W_a)$, where $W_b$ and $W_a$ are the weight of mild steel specimen before and after immersion in test solutions, $W_o$ and $W_i$ are the weight loss of mild steel in the absence and presence of inhibitors respectively, mpy is miles per year, $D$ is the density of the mild steel (7.87 g $cm^{-3}$), $S$ is the area of the specimen ($cm^2$), and $T$ is the period of immersion in hours.

### 2.5. Electrochemical measurements

CH electrochemical analyzer Model 604D was used to record potentiodynamic polarization and electrochemical impedance spectroscopy (EIS) measurements. The working electrode area of 0.5 $cm^2$ mild steel specimen was exposed to 1 M HCl solution. A platinum foil of 3 cm × 3 cm was used as the counter electrode and saturated calomel electrodes were used as reference electrode. All electrochemical measurements were carried out at 308 K using 100 ml of electrolyte (1 M HCl) in stationary condition. Before each electrochemical impedance spectroscopy (EIS) measurement and potentiodynamic polarization (Tafel), the electrode was immersed in test solution at open circuit potential (OCP) for 30 min to be sufficient to attain a stable state. Potentiodynamic polarization curves were recorded from −300 to +300 mV around the OCP with a scan rate of 0.16 mV/s. All the potentials reported were with reference to SCE. The values of related electrochemical corrosion kinetic parameters i.e. corrosion current density ($I_{corr}$), corrosion potential ($E_{corr}$), cathodic and anodic Tafel slopes ($b_c$ and $b_a$) were obtained by extrapolation of the polarization curves. The percentage of inhibition efficiency (% IE) was calculated from $I_{corr}$ values using the following equation:

$$\%IE = \frac{(I_{corr(blank)} - I_{corr(inh)})}{I_{corr(blank)}} \times 100 \quad (3)$$

where $I_{corr(blank)}$ and $I_{corr(inhibitor)}$ are the corrosion current density values without and with an inhibitor.

AC impedance measurements were carried out in the frequency range of 100 kHz to 0.1 Hz with a signal amplitude perturbation of 5 mV. The real part and imaginary part of the cell impedance were measured in ohms for various frequencies. The impedance diagrams are given in Nyquist representation. The inhibition efficiencies for each concentration were calculated using Eq. (4):

$$\%\ IE = \frac{R_{ct(inh)} - R_{ct(blank)}}{R_{ct(inh)}} \times 100 \quad (4)$$

where $R_{ct(blank)}$ and $R_{ct(inh)}$ are the charge transfer resistance in the absence and presence of inhibitor, respectively. All electrochemical tests have been performed in non-de-aerated solutions under unstirred conditions, and the cell temperature was controlled at 308 K using a thermostatic water bath. Each experiment has been repeated three times under the same conditions and the mean values and standard deviations of some parameters such as corrosion current density, Tafel slope and charge transfer resistance are reported.

### 2.6. SEM and EDX analysis

The specimens for surface morphological examination were immersed in 1 M HCl containing optimum concentration of inhibitors (250 ppm) and test solution for 2 h. Then, they were removed, rinsed quickly with acetone and dried. The analysis was performed on a JEOL JSM 6390 scanning electron microscope. The energy of the acceleration beam was employed at 20 keV. Surface analysis of mild steel in 1 M HCl in the absence and the presence of FHLE was performed with a INCA penta FETX3 energy-dispersive X-ray spectrometer.

### 2.7. Diffuse reflectance Fourier Transform-Infrared (DRFT-IR) Spectroscopy

DRFT-IR spectra were recorded using a Bruker Tensor 27 spectrophotometer (resolution 4 $cm^{-1}$). The spectra for FHLE and the protective film formed on the mild steel surface were also measured with DRIFT spectroscopy.

### 2.8. X-ray diffraction (XRD) studies

The mild steel specimens were immersed in 1 M HCl solutions in the absence and presence of optimum concentration (250 ppm) of corrosion inhibitor for a period of 2 h. After 2 h, the specimens were taken out and dried. The nature of the surface film formed on the surface of the mild steel specimen was examined by using XRD-Goniometer (SHIMA DZU-Model XRD 6000).

## 3. Results and discussion

### 3.1. GC–MS analysis

In the present investigation, 9 volatile organic compounds from leaves of *F. hispida* were identified through GC–MS analysis (Fig. 1). The retention time (RT), molecular formula and molecular weight are presented in Table 1. Among the total compounds, Stigmasterol (RT 32.94 with peak area 82.38%) was the major compound identified in the leaf extract. Other notable compounds that are present include 2-(benzyloxyme thyl)-5-methylfuran (0.06%), 2,3 – dihydro-3,5-dihydroxy-6-

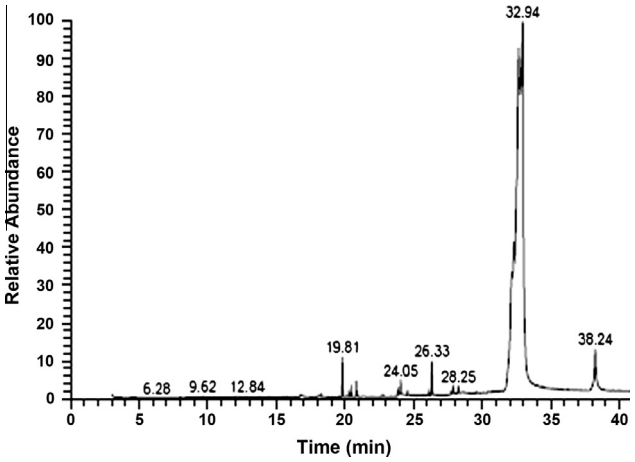


**Figure 1** GC–MS spectrum of FHLE.

**Table 1** Chemical components identified in *Ficus Hispida* leaves extract by GC–MS.

| S. No | RT | Name of the compound | Molecular formula | Molecular weight |
|---|---|---|---|---|
| 1 | 6.28 | 2-(Benzyloxymethyl)-5-methylfuran | $C_{13}H_{14}O_2$ | 202 |
| 2 | 9.62 | 2, 3 – Dihydro -3,5-dihydroxy -6-methyl-pyran-4-one | $C_6H_8O_4$ | 144 |
| 3 | 12.84 | 5-(Hydroxymethyl)-2-Furan carboxaldehyde | $C_6H_6O_3$ | 126 |
| 4 | 19.81 | Neophytadiene | $C_{20}H_{38}$ | 278 |
| 5 | 24.05 | Palmitic acid | $C_{18}H_{36}O_2$ | 284 |
| 6 | 26.33 | Phytol | $C_{20}H_{40}O$ | 296 |
| 7 | 28.25 | Ethyl linoleate | $C_{20}H_{36}O_2$ | 308 |
| 8 | 32.94 | Stigmasterol | $C_{29}H_{48}O$ | 412 |
| 9 | 38.24 | Sitosterols | $C_{29}H_{50}O$ | 414 |

methyl-pyran-4-one (0.12%), 5-(hydroxylmethyl)-2-Furan carboxaldehyde (0.14%), neophytadiene (1.35%), palmitic acid (1.16%), phytol (1.43%), ethyl linoleate (0.34%) and sitosterols (2.91%).

### 3.2. Effect of immersion time

The immersion time is another important parameter in assessing the stability of inhibitive behavior, so it is necessary to evaluate the inhibition efficiency for a long immersion time. In the present study, influence of immersion period (2–24 h) on the inhibition efficiency of the FHLE in 1 M HCl at 308 K was investigated using the weight loss method. Fig. 2 shows the inhibition efficiency obtained in the absence and presence of FHLE which acts as a function of time. Inhibition efficiency is generally lower at shorter exposure time, which means that the adsorption of the extract is gradual and time dependent. On further increasing the immersion period, the amount of FHLE on the surface increases. Thus, the increase in inhibition efficiency observed by weight loss tests from 2 to 12 h is usually due to the decrease of the exposed area because the surface becomes smooth, leading to diminishment of the total surface area. Moreover, the number of $Fe^{2+}$ ions decreases in the solution due to the inhibitor adsorbed on mild steel surface and impede dissolution of mild steel. Maximum inhibition efficiency was reached at 250 ppm FHLE (89.57%) in 1 M HCl for 12 h. Further, as the time of exposure increases beyond 12 h, the overall inhibition efficiency decreases with time. This can be explained by the desorption of FHLE from the surface of mild steel (Karthikaiselvi et al., 2012).

### 3.3. Effect of FHLE on inhibition efficiency

The values of inhibition efficiency obtained from the weight loss for different inhibitor concentrations in 1 M HCl solutions at 308–328 K are shown in Fig. 3. From Fig. 3 it is clear that the inhibition efficiency increased on increasing the FHLE concentration. This behavior could be attributed to the increase in adsorption of the extract at the mild steel/acid interface while increasing the concentration of FHLE. The extract contains oxygen atom in functional groups (C═O, O─H, C═C, C─O) and aromatic moiety (π electron) that is electron rich which can serve as a good adsorption site onto the metal surface thereby inhibiting the corrosion of the mild steel (Hazwan Hussin and Jain Kassim, 2011; Vijayalakshmi et al., 2011; Ezeoke et al., 2012). Naturally occurring products such as *F. Hispida* have carbonyl groups in their molecules through which they can form a inactive layer on the surface of metal which block the active sites of the metal and thus retarded the electrochemical reaction on the metal surface. The extract showed maximum inhibition efficiency of 87.39% in 1 M HCl at an optimum concentration of 250 ppm (308 K). Beyond this concentration, there is no improvement in the inhibition efficiency. This can be attributed to the increase in adsorption of the FHLE molecules onto the mild steel surface. Above 250 ppm, the constant rate could be attributed to the competitive adsorption effect between inhibitor molecules and the metal surface (which is already covered with initial layers of molecules via the initial 200 ppm) and/or the withdrawal of the adsorbed extract to the bulk solution.

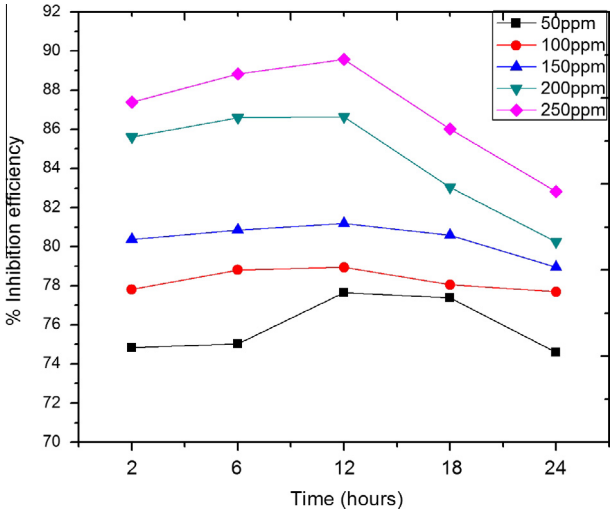


**Figure 2** Variation of inhibition efficiency against time for the corrosion of mild steel in 1 M HCl in the presence of FHLE at 308 K.

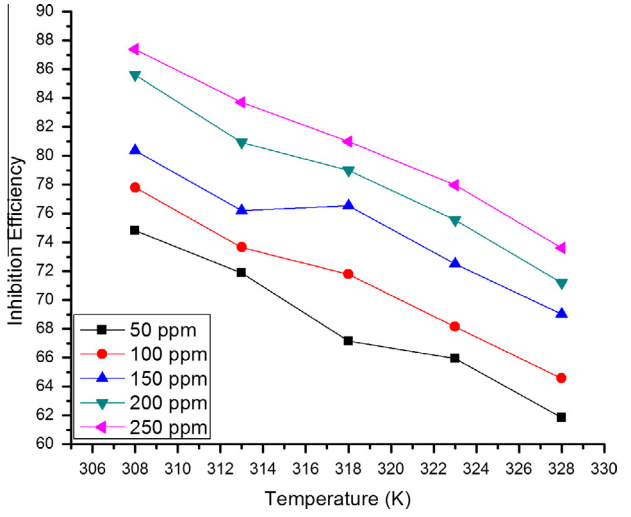


**Figure 3** Effect of temperature on the inhibition efficiency of FHLE concentrations.

The calculated inhibition efficiencies are shown in Fig. 3. From the graph, it is clear that the inhibition efficiency decreased with increase in temperature. This is due to the fact that, at higher temperatures, the mild steel dissolution process is enhanced and the adsorbed inhibitor molecules are partially desorbed from the surface of mild steel (Singh et al., 2011). This gave a clue that the mechanism of adsorption of the inhibitor may be due to physisorption, because the physisorption is due to weak vander Waal's forces, which disappear at elevated temperatures (Shukla and Ebenso, 2011).

### 3.4. Electrochemical impedance spectroscopy (EIS)

EIS is a powerful tool in studying corrosion mechanism and adsorption isotherm (Shivakumar and Mohana, 2012). The effect of inhibitor concentration on the impedance behavior of mild steel in 1 M HCl solution was investigated using this technique. The impedance data are presented as Nyquist and Bode plots in Fig. 4a and b, respectively. The Nyquist plots contain depressed semi-circle with the center under the real axis, whose size is increased by increasing inhibitor concentration, indicating that the corrosion is mainly a charge transfer process (Bentiss et al., 1999). The depressed semicircle is the characteristic of solid electrodes and was often referred to as frequency dispersion which arises due to the substrate roughness and inhomogeneities of the solid surface (Bentiss et al., 2005). It is clear that the impedance response of mild steel has significantly changed after the addition of FHLE in 1 M HCl medium.

The impedance parameters such as solution resistance ($R_s$), charge transfer resistance ($R_{ct}$) and maximum frequency ($f_{max}$) were calculated by ZView software and are given in Table 2. The double layer capacitance ($C_{dl}$) calculated from the following equation is as follows:

$$C_{dl} = \frac{1}{(2\pi \times R_{ct} \times f_{max})} \quad (5)$$

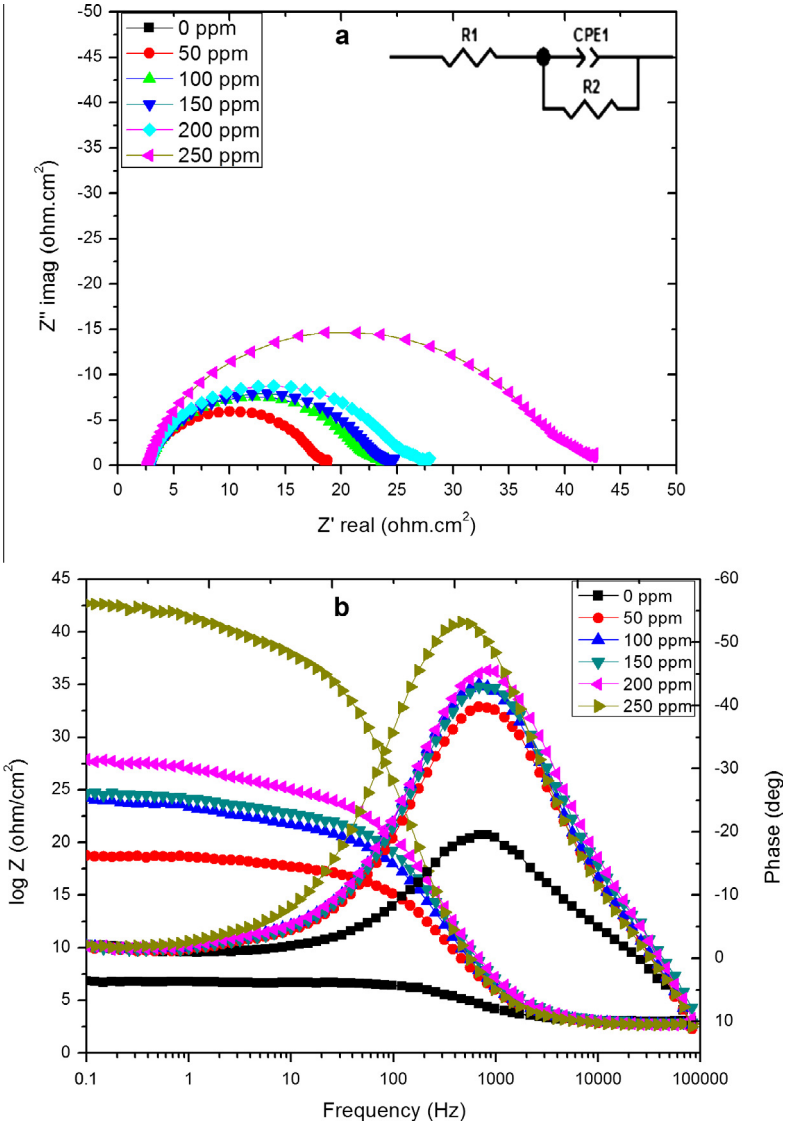


**Figure 4** Nyquist (a) and Bode (b) plots of mild steel in 1 M HCl in the absence and presence of different concentrations of FHLE at 308 K and equivalent circuit used to fit the impedance spectra inserted in it.

**Table 2** Tafel polarization and AC impedance parameters for mild steel in 1 M HCl solutions containing FHLE.

| $C_{inh}$ (ppm) | Tafel polarization | | | | | AC impedance | | |
|---|---|---|---|---|---|---|---|---|
| | $-E_{corr}$ (mV) | $i_{corr}$ (μA cm$^{-2}$) | $-b_c$ (mV/decade) | $-b_a$ (mV/decade) | % IE | $R_{ct}$ (Ω cm$^2$) | $C_{dl}$ (F/cm$^2$) | % IE |
| 0 | 487 | 1329 | 197.04 | 140.64 | – | 3.814 | $8.54 \times 10^{-3}$ | – |
| 50 | 502 | 827.5 | 222.02 | 107.03 | 37.73 | 15.64 | $9.65 \times 10^{-4}$ | 75.61 |
| 100 | 525 | 242.8 | 191.16 | 92.44 | 81.73 | 20.92 | $5.88 \times 10^{-4}$ | 81.76 |
| 150 | 528 | 74.13 | 259.74 | 84.33 | 94.42 | 21.14 | $5.61 \times 10^{-4}$ | 81.95 |
| 200 | 547 | 65.27 | 209.90 | 53.27 | 95.08 | 24.80 | $4.36 \times 10^{-4}$ | 84.62 |
| 250 | 537 | 56.91 | 257.06 | 71.10 | 95.71 | 39.27 | $1.84 \times 10^{-4}$ | 90.29 |

where $f_{max}$ is the frequency at the maximum on the Nyquist plot. As seen from Table 2, the $R_{ct}$ values increased with the increasing concentration of the inhibitor. On the other hand, the value of $C_{dl}$ decreased with an increase in inhibitor concentration. This decrease is due to the decrease in local dielectric constant and/or increase in thickness of the electrical double layer, suggesting that the FHLE acts via adsorption at the metal/solution interface (Khaled, 2003; Behpour et al., 2008). It could be assumed that the decrease of $C_{dl}$ values is caused by the gradual replacement of water molecules by adsorption of organic molecules on the electrode surface, which decreases the extent of the metal dissolution (Khaled, 2003).

The obtained EIS data were fitted to the electrical equivalent circuit diagram given in Fig. 4a in order to model of mild steel/solution interface in the absence and presence of the inhibitor. The circuit employed allows the identification of both solution resistance ($R_s$) and charge transfer resistance ($R_{ct}$). It is worth mentioning that the double layer capacitance ($C_{dl}$) value is affected by imperfections of the surface and that this effect is simulated via a constant phase element (CPE). The CPE contains the component $Q_{dl}$ and the coefficient α that quantifies different physical phenomena such as surface inhomogeneousness resulting from surface roughness, inhibitor adsorption, and porous layer formation. Therefore, the capacitance is deduced from the following relation:

$$C_{dl} = Q_{dl} \times (2\pi f_{max})^{\alpha-1} \quad (6)$$

A parallel combination of capacitance and resistance as a series to the circuit of cathodic branch as a charge transfer resistance with parallel charge transfer resistance–diffusional impedance for the anodic branch. The circuit after solution resistance is attributed to the passive film, which formed on the metal surface. Fig. 4b shows the Bode impedance magnitude and phase angle plots recorded for the mild steel electrode immersed in 1 M HCl in the absence and presence of various concentration of FHLE at its OCP. An ideal capacitive behavior would result if a slope value attains −1 and a phase angle value attains −90° (Naderi et al., 2009). In the medium frequency zone, a linear relationship between log |Z| vs. log *f* with a slope near −0.1 and the phase angle approaching −55° has been observed (Fig. 4b). This is a characteristic response to capacitive behavior in the medium frequency zone. The slope values of Bode impedance magnitude plots in the medium frequency zone, G and the maximum phase angle, α, exhibited aberrations from the values of −1° and −90°, respectively. These aberrations are considered to be from the ideal capacitive response at intermediate frequencies. The Bode phase angle plots exhibit one time constant (single maximum) at intermediate frequencies, and broadening of this maximum in the presence of FHLE accounts for the formation of a protective layer on the electrode surface (Hassan, 2007).

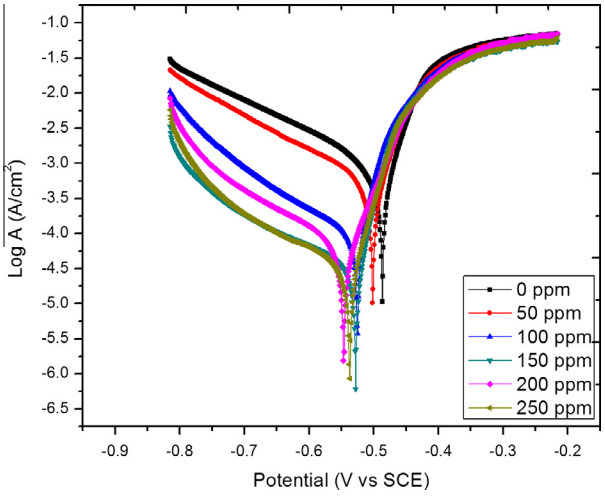


**Figure 5** Polarization curves for mild steel in 1 M HCl with different concentrations of FHLE at 308 K.

### 3.5. Potentiodynamic polarization studies

Fig. 5 shows the cathodic and anodic polarization plots of mild steel immersed in 1 M HCl at 308 K in the absence and presence of different concentrations of FHLE. It is evident from Fig. 5 that both reactions were suppressed with the addition of FHLE used in the study, suggesting that FHLE reduced the anodic dissolution reactions and retarded the hydrogen evolution reactions on the cathodic sites. Electrochemical parameters such as corrosion potential ($E_{corr}$), cathodic and anodic Tafel slopes ($b_c$ and $b_a$) and corrosion current density ($I_{corr}$) were obtained by extrapolation of the anodic and cathodic regions of the Tafel plots and inhibition efficiency is listed in Table 2. It is evident from Table 2 that the value of $b_a$ changed with increase in the presence of FHLE whereas more pronounced change occurs in the values of $b_c$ indicating that both anodic and cathodic reactions are effected but effect on the cathodic reactions is more prominent. The shift in the anodic Tafel slope ($b_a$) is due to the inhibitor molecules adsorbed on the metal surface. An inhibitor can be classified as an anodic or cathodic type when the change in $E_{corr}$ value is larger than 85 mV (Li et al., 2008). In the present study, the maximum displacement was 60 mV cathodically when compared to the

blank. This indicates that the FHLE reduces the corrosion rates predominantly by hydrogen evolution of mild steel.

The data in Table 2 show that increasing FHLE concentration, the values of corrosion potential ($E_{corr}$) shifted to negative direction indicating that it acts as mixed type inhibitor, but predominantly cathodic. The obtained results show that the inhibition efficiency increased, while the corrosion current density ($I_{corr}$) decreased when the concentration of FHLE is increased. This could be explained on the basis of adsorption of FHLE on the mild steel surface and the adsorption process increased with enhancing inhibitor concentration and also hindered attack on the mild steel electrode by acid.

The results of electrochemical measurements agreed well with those of weight loss studies with the slight deviation in the values. Variation in the immersion period of mild steel in 1 M HCl is the reason for the observed deviation.

### 3.6. Activation parameters

The apparent activation energy ($E_a$), the enthalpy of activation ($\Delta H^*$) and the entropy of activation ($\Delta S^*$) for the corrosion of mild steel specimens in 1 M HCl solutions in the absence and presence of different concentrations of FHLE at 308–328 K were calculated from Arrhenius equation:

$$\log CR = \log A - E_a/2.303RT \quad (7)$$

and transition-state equation:

$$\log\left(\frac{CR}{T}\right) = \log\left(\frac{R}{hN}\right) + \left(\frac{\Delta S^*}{2.303R}\right) - \left(\frac{\Delta H^*}{2.303RT}\right) \quad (8)$$

where $CR$ is the corrosion rate, $A$ is the pre-exponential factor, $h$ is the Planck's constant, $N$ is the Avogadro's number, $E_a$ is the apparent activation energy, $R$ is the gas constant ($R = 8.314\ \mathrm{J\ mol^{-1}\ K^{-1}}$) and $T$ is the absolute temperature.

A plot of log $CR$ vs $1/T$ (Fig. 6) and log $CR/T$ vs $1/T$ (Fig. 7) gave straight line with slope of $-E_a/2.303R$ and $-\Delta H^*/2.303R$, respectively. The intercept which is calculated will be log $A$ and log $R/hN + (\Delta S^*/2.303R)$ for Arrhenius and transition-state equations respectively. The calculated values of the apparent activation energy ($E_a$), the enthalpy of activation ($\Delta H^*$) and the entropy of activation ($\Delta S^*$) are given in Table 3. It shows that the values of $E_a$ for inhibited solutions ranged from 70.65 to 83.33 kJ/mol. The value of $E_a$ found for FHLE is higher than that obtained for 1 M HCl solution. It is often interpreted by physical adsorption leading to the formation of an adsorptive film of electrostatic character. The apparent activation energy increased with increasing concentration of FHLE as a result of the appreciable decrease in adsorption of the inhibitor on the mild steel surface with increase of temperature and corresponding increase in the reaction rate because of the greater area of mild steel that is exposed to hydrochloric acid (Sobhi et al., 2011). Inhibitors may be classified into three groups according to the temperature effects (Radovici, 1965). In the present study, the decrease in % IE with rise in temperature, with accordant increase in corrosion activation energy in the presence of FHLE compared with that in its absence, is good evidence for a physical mechanism of FHLE on the mild steel surface (Povova et al., 2003). The obtained results indicate that FHLE acted as inhibitors through increasing activation energy of mild steel dissolution by making a barrier to mass and charge transfer by their adsorption on the mild steel surface. The positive sign of $\Delta H^*$ reflects endothermic nature of the mild steel dissolution process and it needs more energy to achieve the active state or equilibrium state (Bouklah et al., 2006; Wahyuningrum et al., 2008). From Table 3, it is clear that entropy of activation

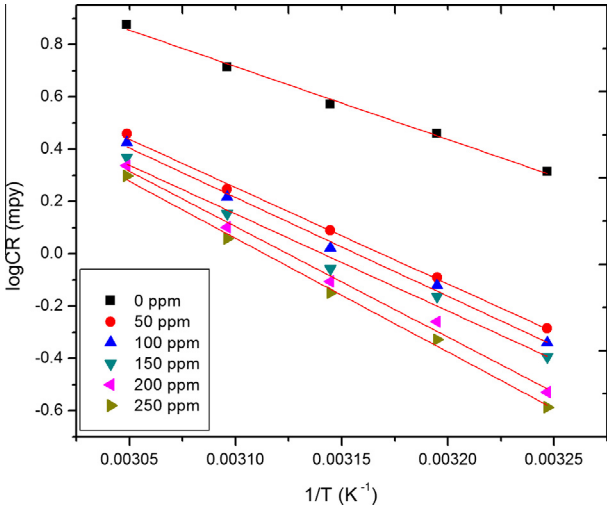


**Figure 6** Arrhenius plots for log CR vs $1/T$ for steel in 1 M HCl at different concentrations of FHLE.

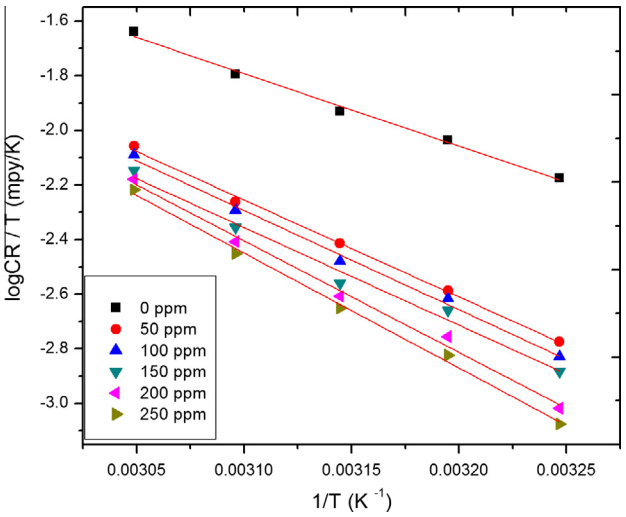


**Figure 7** The relationship between log $CR/T$ vs $1/T$ for mild steel at different concentrations of FHLE.

**Table 3** Activation parameters of mild steel in 1 M HCl in the absence and presence of FHLE.

| Concentrations of FHLE (ppm) | $E_a$ (kJ/mol) | $\Delta H^*$ (kJ/mol) | $\Delta S^*$ (J mol$^{-1}$ K$^{-1}$) |
|---|---|---|---|
| 0 | 53.40 | 50.76 | −74.49 |
| 50 | 70.65 | 68.01 | −29.90 |
| 100 | 72.34 | 69.69 | −25.36 |
| 150 | 71.15 | 68.51 | −30.24 |
| 200 | 80.97 | 78.33 | −0.93 |
| 250 | 83.33 | 80.69 | 5.57 |

increased in the presence of FHLE compared to the 1 M HCl solution. In the free acid solution it can be explained as follows: the transition state of the rate determining recombination step represents a more orderly arrangement relative to the initial state, so a high value for the entropy of activation is obtained. In the presence of inhibitor, however, the rate determining step is the discharge of hydrogen ions to form adsorbed hydrogen atoms. Since the surface is covered with the inhibitor molecules, this will retard the discharge of hydrogen ions on the metal surface causing the system to pass from a random arrangement, and hence entropy of activation is increased. Hence, increase in the entropy of activation ($\Delta S^{*}$) in the presence of inhibitor increases in the disordering on going from reactant to activated complex (Shukla and Ebenso, 2011).

### 3.7. Adsorption isotherms

The mechanism of corrosion inhibition may be explained on the basis of adsorption behavior. The degree of surface coverage ($\theta$) for different inhibitor concentrations was evaluated by weight loss data. The experimental data were applied to various adsorption isotherms including Freundlich, Frumkin, Langmuir, Temkin and Flory–Huggins isotherms. A correlation between the surface coverage ($\theta$) and the inhibitor concentration ($C$) in an electrolyte can be represented by the Langmuir adsorption isotherm:

$$\frac{C}{\theta} = \frac{1}{K_{ads}} + C \tag{9}$$

where $C$ is the concentration of inhibitor (ppm), $K_{ads}$ is the adsorption–desorption equilibrium constant and $\theta$ is the surface coverage which is given as

$$\theta = \frac{\%\ \mathrm{IE}}{100} \tag{10}$$

Straight lines were obtained when $C/\theta$ was plotted against $C$ (g/l) (Fig. 8). The linear relationships suggested that the adsorption of inhibitors obeyed Langmuir adsorption isotherm. From the intercept of the straight lines, the values of $K_{ads}$ were calculated and are summarized in Table 4. The standard free energy of adsorption $\left(\Delta G^{o}_{ads}\right)$ and the equilibrium constant ($K_{ads}$) are related by the following equation:

$$\Delta G^{o}_{ads} = -RT\ln(55.5 \times K_{ads}) \tag{11}$$

where $R$ is the gas constant, $T$ is the temperature and 55.5 is the molar concentration of water in solution. The values of $K_{ads}$ were found to decrease with increasing temperature showing that the interactions between the adsorbed molecules and the metal surface are weakened and the inhibitor molecules become easily removable. Such data explain the decrease in the protection efficiency with an increasing temperature. The negative values of $\left(\Delta G^{o}_{ads}\right)$ clearly indicated that spontaneous adsorption of FHLE on mild steel surface took place through physical adsorption mechanism. In the present investigation the calculated values of $\left(\Delta G^{o}_{ads}\right)$ around −20 kJ/mol, indicating that the adsorption mechanism of FHLE in 1 M HCl solution at the studied temperatures may be a physisorption, which was consistent with electrostatic interaction between a charged molecule and a charged metal (Umoren et al., 2009; Solomon et al., 2010).

The heat of adsorption and entropy of adsorption are important parameters for understanding the adsorption of an organic inhibitors at metal/solution interface. The heat of adsorption ($\Delta H_{ads}$) is calculated using the van't Hoff equation:

$$\ln K_{ads} = \frac{-\Delta H_{ads}}{RT} + \text{constant} \tag{12}$$

**Table 4** Thermodynamic parameters for the adsorption of FHLE on the mild steel in 1 M HCl solutions.

| Temperature (K) | $K_{ads}$ (L/g) | $-\Delta G^{o}_{ads}$ (kJ/mol) | $\Delta H_{ads}$ (kJ/mol) | $\Delta S_{ads}$ (J mol$^{-1}$ K$^{-1}$) | $R^2$ |
|---|---|---|---|---|---|
| 308 | 58.82 | 20.71 | | 38.46 | 0.997 |
| 313 | 55.55 | 20.90 | | 38.45 | 0.996 |
| 318 | 52.63 | 21.09 | −8.871 | 38.44 | 0.999 |
| 323 | 50.00 | 21.29 | | 38.45 | 0.997 |
| 328 | 47.61 | 21.48 | | 38.46 | 0.998 |

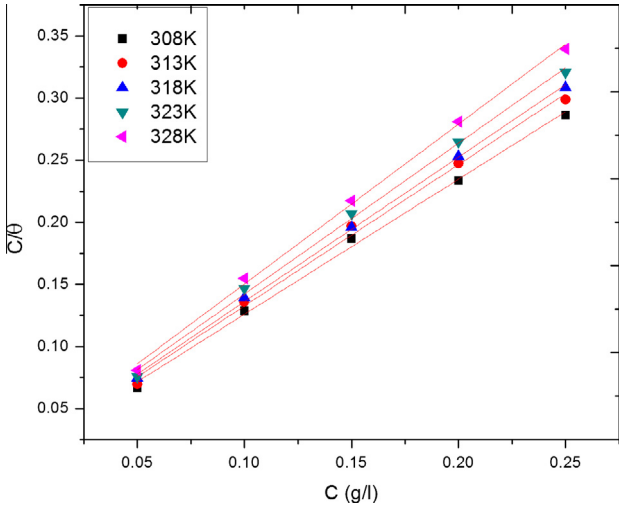


**Figure 8** Langmuir adsorption isotherm for mild steel in 1 M HCl containing different concentrations of FHLE at 308–328 K.

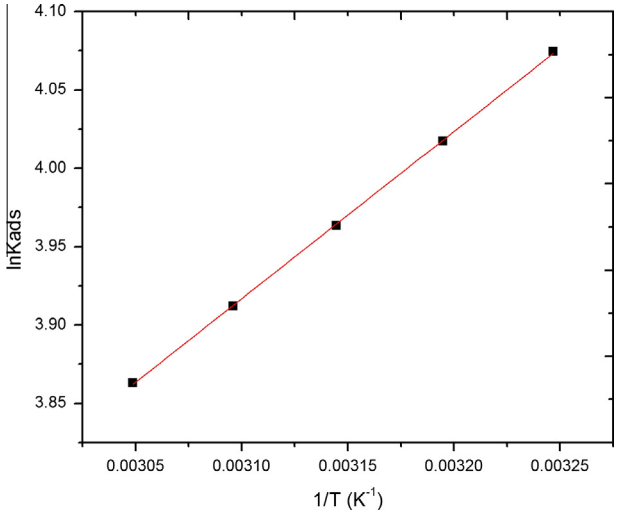


**Figure 9** Plot of ln $K_{ads}$ versus $1/T$ for the adsorption of FHLE at mild steel/HCl interface.

Fig. 9 shows the straight lines of plot of $\ln K_{ads}$ vs $1/T$ and slope of this straight line is equal to $-\Delta H_{ads}/R$. The heat of adsorption could be approximately regarded as the standard heat of adsorption ($\Delta H_{ads}$) under experimental conditions. Now standard entropy of adsorption ($\Delta S_{ads}$) is obtained by the thermodynamic basic equation:

$$\Delta S_{ads} = \frac{\Delta H_{ads} - \Delta G^{o}_{ads}}{T} \quad (13)$$

All the calculated thermodynamic parameters are listed in Table 4. Values of $\Delta H_{ads}$ were negative, suggesting that the adsorption of inhibitor is an exothermic process, which means that the efficiency inhibition is lower at high temperature, as a result of gradual desorption of the inhibitor from the mild steel surface (Li et al., 2012). The values of entropy of adsorption of FHLE on mild steel in 1 M HCl are positive and large (Table 4), which indicates the increase of disorder due to the adsorption of the inhibitor molecules by desorption of more water molecules (Saleh, 2006).

### 3.8. SEM and EDX analysis

SEM images of polished mild steel surface, mild steel immersed in 1 M HCl in the absence and presence of FHLE are shown Fig. 10a–c. Close examination of the SEM images revealed that the specimens immersed in the inhibitor solutions are in better conditions with smooth surfaces when compared with those of corroded rough and coarse uneven surfaces of mild steel immersed in 1 M HCl alone. This observation indicated that corrosion rate is remarkably decreased in the presence of the inhibitors. This might be due to the adsorption of inhibitor molecules on the metal surface as a protective layer.

The corresponding protective film formed on a polished metal surface was examined using an EDX analysis. The spectrum of the polished mild steel surface after immersion in 1 M HCl solution in the absence and presence of the inhibitor is shown in Fig. 11a–c, respectively. Fig. 11a and Table 5 indicate the EDX spectrum of mild steel, which revealed that the surface was chlorine free in the absence of 1 M HCl solution. But in the case of mild steel with hydrochloric acid solution, Fig. 11b shows the mild steel surface contains mainly Fe and O with small quantities of Cl (Table 5 & Fig. 11a). This indicates that the corrosion of iron took place through the formation of iron chlorides and/or iron oxides. On the other hand, the elements found in the protective layer obtained by EDX in the presence of FHLE inhibitor were carbon, oxygen and iron (Fig. 11c). The detection of carbon, oxygen and iron on the surface indicates unquestionably the presence of FHLE molecules on the mild steel surface. The oxygen peak which appears in EDX spectra (Fig. 11c) is due to the fact that inhibitor contains oxygen atom and it coordinated with Fe. The appearance of carbon in the EDX profile confirms that FHLE molecules adsorbed on mild steel surface and it prevents the corrosion of iron through its adsorption on the surface blocking its weak damages and preventing the formation of ferric and ferrous chloride compounds. The percentage of atomic contents of elements on the mild steel surface after exposure to 1 M HCl solution with and without FHLE is shown in Table 5.

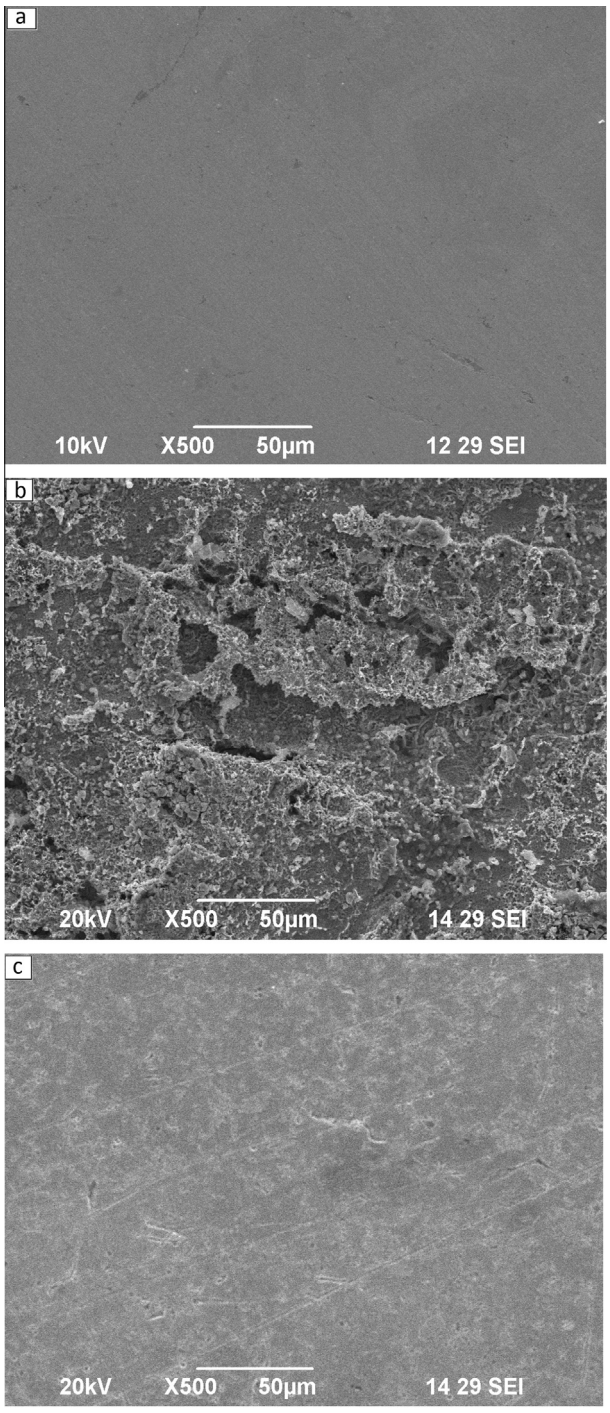


**Figure 10** SEM images of (a) Polished mild steel surface, (b) after 2 h of immersion at 308 K in 1 M HCl and (c) after 2 h of immersion at 308 K in 1 M HCl + FHLE.

### 3.9. DRFT-IR studies

The diffuse reflectance adsorption FTIR spectra of the surface films formed on mild steel in the absence and presence of the inhibitor formulation are shown in Fig. 12. In the FTIR spectrum of pure FHLE, original absorption band at 3313 $cm^{-1}$ is attributed to the strong stretching mode of O—H. The

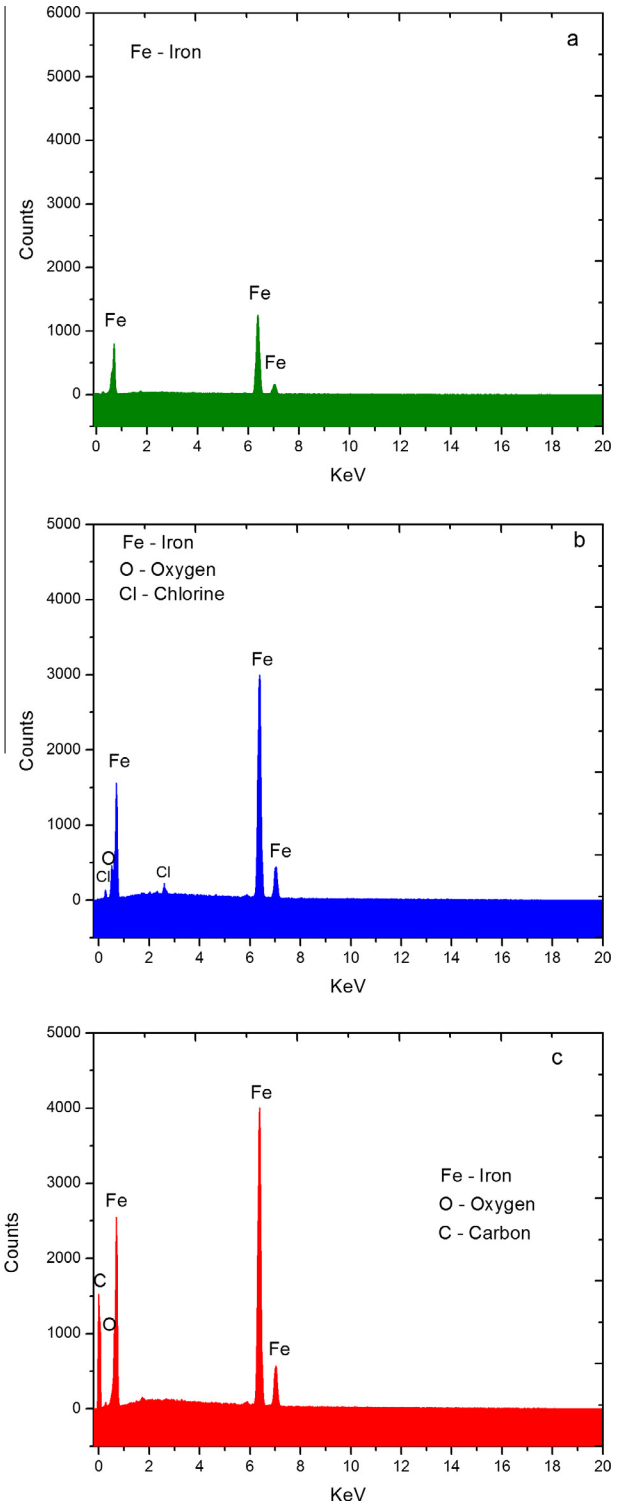


**Figure 11** EDX spectra of (a) Polished mild steel surface, (b) mild steel exposed in 1 M HCl and (c) mild steel exposed in 1 M HCl in the presence of FHLE.

spectrum of FHLE mainly showed the band at 1644 $cm^{-1}$ is due to the C═O stretching vibrations and the peak at 2934 $cm^{-1}$ is related to the $CH_2$ asymmetrical stretching vibrations. The band at 1415 $cm^{-1}$ is due to the stretching mode of $CH_2$ bending vibration in $CH_3$ (Deng and Li, 2012). The peak at 1034 $cm^{-1}$ corresponds to the C—O stretching vibrations.

**Table 5** EDX analysis of mild steel in 1 M HCl in the absence and presence of FHLE.

| Medium | Composition | | | |
|---|---|---|---|---|
| | Fe | O | Cl | C |
| Polished (a) | 100 | – | – | – |
| 1 M HCl (b) | 73.64 | 22.79 | 3.57 | – |
| *Ficus hispida* (c) | 91.65 | 4.22 | – | 4.13 |

The FT-IR spectrum of adsorbed protective layer formed on mild steel surface after immersion in 1 M HCl containing 250 ppm of FHLE is shown in Fig. 12b. On comparing Fig. 12a & b, all important peaks present in pure compound appear in adsorption layer on the steel surface, which means that most of the functional groups in FHLE are present in the adsorbed surface film. Moreover, some of the peaks for the adsorbed film have diminished or even vanished. The spectrum of the FHLE adsorbed surface films (the O—H stretching frequencies around 3400 $cm^{-1}$, the C—H stretching frequencies at 2923 $cm^{-1}$ and the C—O stretch around 1100 $cm^{-1}$) suggests that these functional groups are directly involved in iron-inhibitor interactions, thus confirming the proposed adsorption of some organic constituents of FHLE on the mild steel.

### 3.10. X-ray diffraction analysis

The X-ray diffraction patterns of the surface of the mild steel specimens immersed in the test solutions are given in Fig. 13. The patterns obtained clearly reveal the presence of metal and metal oxide phases. A series of characteristics peaks at 35.2 (104), 44.6 (110), 64.9 (200), 82.2 (211) and 98.9 (220) are observed and they are in accordance with the standard Fe and $FeCl_2$ patterns (JCPDS: 06-0696). Peak at $2\theta = 35.2°$ can be assigned to chlorides of iron. The peak due to iron appears at $2\theta = 44.6°$, 64.9°, 82.2° and 98.9° (Fig. 13a). It is seen here that the surface of the metal immersed in 1 M HCl alone contains $FeCl_2$. But in the presence of FHLE, the intensity of the peaks due to iron alone is observed at $2\theta = 44.6°$, 82.2°, 98.9° which are very high (Fig. 13b). It therefore, appears from the very weak diffraction intensities obtained in this range that there should be a very small amount of iron oxides present in the corrosion product which is in support of corrosion inhibition. The formation of adsorbed protective film on the surface of metal in the presence of FHLE is clearly reflected from these observations. This method may be useful to complete interaction of inhibitor with metallic surface (Govindaraju et al., 2009).

### 3.11. Explanation of corrosion inhibition

GC–MS analysis of leaf extract leads to the identification of 9 phytochemical constituents. It is interesting to see here that the ethanol extract of *F. Hispida* leaves contains oxygen and π electrons in their molecules. Moreover, the previous studies on the phytochemical constituents of the leaf extract show that FHLE contains a mixture of organic compounds containing O and/or π-electrons in their molecules (Sirisha et al., 2010). However, the highly complex chemical compositions of the plant extracts make it rather difficult to assign the inhibitive effect to a particular compound present in the leaf extract.

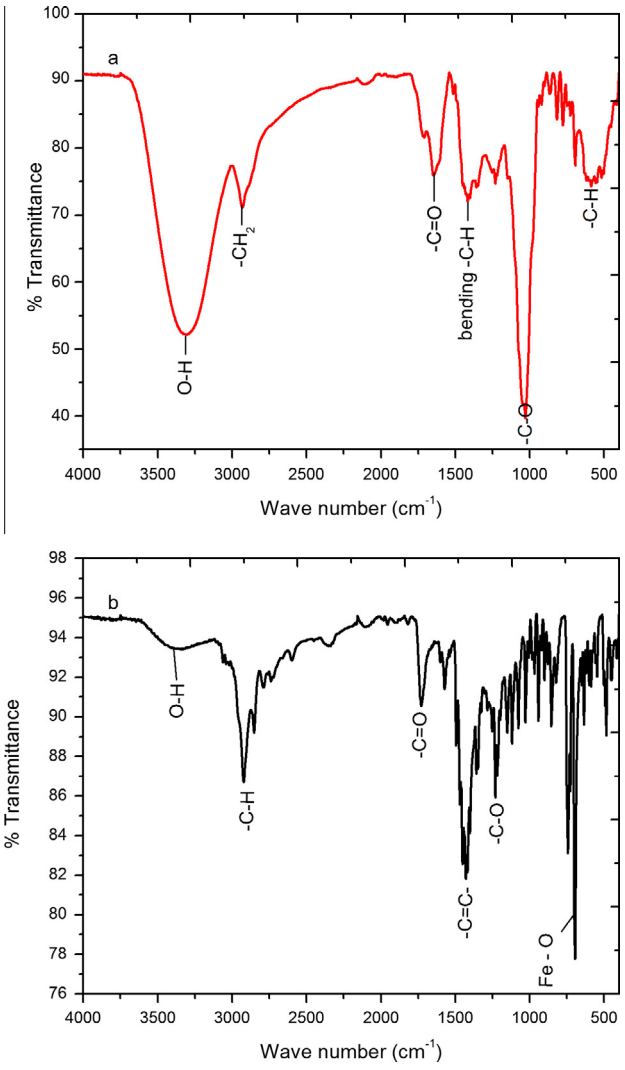


**Figure 12** (a) DRFT-IR spectra of FHLE and (b) DRFT-IR spectra of surface film of the mild steel specimen after immersion in 1 M HCl containing FHLE.

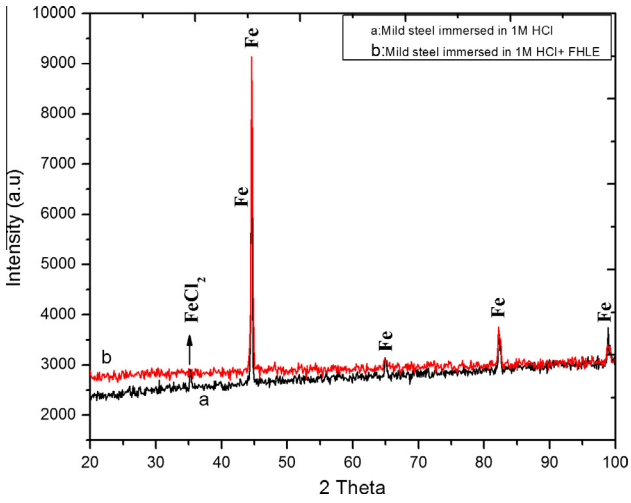


**Figure 13** XRD pattern of (a) mild steel in 1 M HCl and (b) mild steel in 1 M HCl in the presence of FHLE.

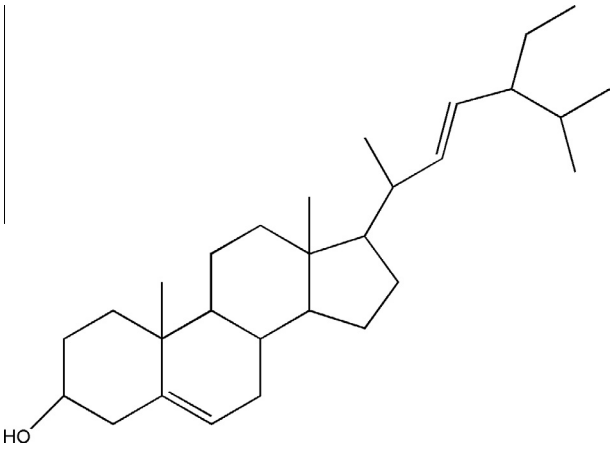


**Figure 14** Chemical structure of stigmasterol.

The first stage in the action mechanism of inhibitor in acid media is adsorption on the metal surface (Yurt et al., 2004). This indicates that the inhibition efficiency of the extract is due to the presence of some or all of the above listed phytochemical constituents (Table 1). The adsorption of the inhibitor molecules on the mild steel surface is due to the donor–acceptor interaction between electrons of donor atoms oxygen and the acceptor, i.e., vacant d orbital of iron surface atoms. The inhibitor molecules can also adsorb on the metal surface in the form of negatively charged species which can interact electrostatically with positively charged metal surface, which leads to increase the surface coverage and consequently protect efficiency even in the case of low inhibitor concentration. This assumption could be further confirmed by the FTIR results that *F. hispida* leaves extract could adsorb onto steel surface to form a dense and more tightly protective film covering both cathodic and anodic reaction sites and, thus, retarding corrosion phenomenon.

The basic requirements for inhibitors to show an excellent inhibition power are as follows (Eddy et al., 2011):

(i) Presence of suitable functional groups (i.e. π-electron rich functional systems).
(ii) Presence of hetero atoms in the compound.
(iii) Presence of conjugated system.
(iv) Possession of aromatic ring or long carbon chain that has hetero atom.

From Table 1, it is evident that all the compounds in FHLE meet all the above mentioned conditions. The main constituent of *F. hispida* leaves extract is stigmasterol whose structures are given in Fig. 14. Inspection of Fig. 14 reveals that the compounds contained in the leaf extract of *F. hispida* are sterol molecules with attached OH group in one direction and a hydrocarbon chain at the opposite direction. The presence of attached O atoms may be responsible for the adsorption of such compounds on the metal surface. Therefore, the compounds are adsorbed on the metal surface through the lone pair of electrons present on the oxygen atom while the rest of molecule is oriented toward the solution. Hydrocarbon chains repel the aqueous acidic solution out of the electrode surface leading to inhibition of the attack of the aggressive solution on the metal surface.

Please cite this article in press as: Muthukrishnan, P. et al., Stigmasterol extracted from *Ficus hispida* leaves as a green inhibitor for the mild steel corrosion in 1 M HCl solution. Arabian Journal of Chemistry (2015), http://dx.doi.org/10.1016/j.arabjc.2015.09.005

## 4. Conclusion

The following main conclusions are drawn from this study. The inhibition efficiency of FHLE decreases with rise in temperature and its decrease leads to increased activation energy of the corrosion process, which suggests a physical adsorption mechanism. Potentiodynamic polarization measurements demonstrate that FHLE acts as a mixed type inhibition with cathodic its dominant. The results of EIS indicate that the double layer capacitance decreases with respect to the acid solution when the FHLE is added. The adsorption of FHLE on the mild steel surface follows the Langmuir adsorption isotherm. The free energy of adsorption $\Delta G^{o}_{ads}$ indicates that the process was spontaneous and physically adsorbed (Physisorption) onto the mild steel surface. Surface analysis shows that there were some improvements on the surface morphology after being added with the inhibitor. The corrosion inhibition is primarily due to the presence of stigmasterol. The other constituents may synergistically increase the strength of the film formed on the metal surface.

## References

Abdel Gaber, A.M., Abd-El-Nabey, B.A., Saadawy, M., 2009. Corros. Sci. 51, 1038–1042.
ASTM G 31-72, 1990. Standard Practice for Laboratory Immersion Corrosion Testing of Metals. ASTM, West Conshohocken, PA.
Ating, E.I., Umoren, S.A., Udousoro, I.I., Ebenso, E.E., Udoh, A.P., 2010. Green Chem. Lett. Rev. 3, 61–68.
Bentiss, F., Lagrenee, M., Traisnel, M., Hornez, J.C., 1999. Corros. Sci. 41, 789–803.
Bentiss, F., Lebrini, M., Lagrenee, M., 2005. Corros. Sci. 47, 2915–2931.
Behpour, M., Ghoreishi, S.M., Soltani, N., Salavati-Niasari, M., Hamadanian, M., Gandomi, A., 2008. Corros. Sci. 50, 2172–2181.
Bouklah, M., Benchat, N., Hammouti, B., Aouniti, A., Kertit, S., 2006. Mater. Lett. 60, 1901–1905.
Cardozo da Rocha, J., da Cunha, Antonio., Ponciano Gomes, J., Elia, E.D., 2010. Corros. Sci. 52, 2341–2348.
Deng, S.D., Li, X.H., 2012. Corros. Sci. 55, 407–415.
Eddy, N.O., Ameh, P., Gimba, C.E., Ebenso, E.E., 2011. Int. J. Electrochem. Sci. 6, 5815–5829.
El-Etre, A.Y., 2007. J. Colloid Interface Sci. 314, 578–583.
Ezeoke, A.U., Obi-Egbedi, N.O., Adeosun, C.B., Adeyemi, O.G., 2012. Int. J. Electrochem. Sci. 7, 5339–5355.
Ghosh, R., Sharatchandra, Kh., Rita, S., Thokchom, I.S., 2004. Indian J. Pharmacol. 36, 222–225.
Govindaraju, K.M., Gobi, D., Kavitha, L., 2009. J. Appl. Electrochem. 39, 2345–2352.
Hassan, H.H., 2007. Electrochim. Acta 53, 1722–1730.
Hazwan Hussin, M., Jain Kassim, M., 2011. Int. J. Electrochem. Sci. 6, 1396–1414.
Issaadi, S., Douadi, T., Zouaoui, A., Chafaa, S., Khan, M.A., Bouet, G., 2011. Corros. Sci. 53, 1484–1488.
Kamal, C., Sethuraman, M.G., 2012. Ind. Eng. Chem. Res. 51, 10399–10407.
Karthikaiselvi, R., Subhashini, S., Rajalakshmi, R., 2012. Arabian J. Chem. 5, 517–522.
Khaled, K.F., 2003. Electrochim. Acta 48, 2493–2503.
Li, W., He, Q., Zhang, S., Pei, C., Hou, B., 2008. J. Appl. ElectroChem. 38, 289–295.
Li, X., Deng, S., Fu, H., 2012. Corros. Sci. 62, 163–175.
Muthukrishnan, P., Jeyaprabha, B., Tharmaraj, P., Prakash, P., 2014a. Res. Chem. Intermed., 5961–5984
Muthukrishnan, P., Jeyaprabha, B., Prakash, P., 2013a. Acta Metall. Sin. (Engl. Lett.) 26, 416–424.
Muthukrishnan, P., Jeyaprabha, B., Prakash, P., 2013b. Arabian J. Chem., http://dxdoi.org/10.1016/j.arabjc.2013.08.011.
Muthukrishnan, P., Jeyaprabha, B., Prakash, P., 2013c. J. Mater. Eng. Perform. 22, 3792–3800.
Muthukrishnan, P., Jeyaprabha, B., Prakash, P., 2014b. Int. J. Ind. Chem. 5. http://dx.doi.org/10.1007/s 40090-014-0005-9.
Muthukrishnan, P., Saravana Kumar, K., Jeyaprabha, B., Prakash, P., 2014c. Metall Mater. Trans. 45, 4510–4524.
Muthukrishnan, P., Karthik, R., Jeyaprabha, B., Prakash, P., 2014d. Int. J. Miner, Metall. Mater. 21, 1083–1095.
Naderi, E., Jafari, A.H., Ehteshamzadeh, M., Hosseini, M.G., 2009. Mater. Chem. Phys. 115, 852–858.
Oguize, E.E., 2006. Mater. Chem. Phys. 99, 441–446.
Orubite, K.O., Oforka, N.C., 2004. Mater. Lett. 58, 1768–1772.
Peraza-Sanchez, S.R., Chai, H.B., Shin, Y.G., Santisuk, T., Reutrakul, V., Fransworth, N.R., Cordell, G.A., Pezzuto, J.M., Kinghorn, A. D., 2002. Planta Med. 68, 186–188.
Popova, A., Sokolova, E., Raicheva, S., Christov, M., 2003. Corros. Sci. 45, 33–58.
Quraishi, M.A., Khan, M.A.W., Ajmal, M., Muralitharan, S., Iyer, S. V., 1997. Br. Corros. J. 53, 475–480.
Radovici, O., 1965. In: Proceedings of the 2nd European Symposium on Corrosion Inhibitors, Ferrara, pp. 178.
Saleh, M.M., 2006. Mater. Chem. Phys. 98, 83–89.
Shanmugarajan, T.S., Arunsundar, M., Somasundaram, I., Krishnakumar, E., Sivaraman, D., Ravichandran, V., 2008a. Int. J. Pharmacol. 4, 78–87.
Shanmugarajan, T.S., Arunsundar, M., Somasundaram, I., Sivaraman, D., Krishna kumar, E., Ravichandran, V., 2008b. J. Pharmacol. Toxicol. 4 (2), 363–372.
Shukla, S.K., Ebenso, E.E., 2011. Int. J. Electrochem. Sci. 6, 3277–3291.
Solmaza, R., Altunbas, E., Kardas, G., 2011. Mater. Chem. Phys. 125, 796–801.
Soltani, N., Behpour, M., Ghoreishi, S.M., Naeimi, H., 2010. Corros. Sci. 52, 1351–1361.
Singh, A., Ahamad, I., Singh, V.K., Quraishi, M.A., 2011. J. Solid State Electrochem. 15, 1087–1097.
Shivakumar, S.S., Mohana, K.N.S., 2012. Eur. J. Chem. 3, 426–432.
Sirisha, N., Sreenivasulu, M., Sangeetha, K., Madhusudhana chetty, C., 2010. Int. J. Pharm. Tech. Res. 2, 2174–2182.
Sobhi, M., Abdallah, M., Khairou, K.S., 2011. Monatsh. Chem. 143, 1379–1388.
Solomon, M.M., Umoren, S.A., Udosoro, I.I., Udoh, A.P., 2010. Corros. Sci. 52, 1317–1325.
Subhash, C., Mandal, C.K., Ashok, K., 2002. Fitoterapia 73, 663–667.
Umoren, S.A., Obota, I.B., Ebenso, E.E., Obi-Egbedi, N.O., 2009. Desalination 247, 561–572.
Vijayalakshmi, P.R., Rajalakshmi, R., Subhashini, S., 2011. Portug. Electrochim. Acta 29, 9–21.
Wahyuningrum, D., Achmad, S., Syah, Y.M., Buchari, Bundjali B., Ariwahjoedi, B., 2008. Int. J. Electrochem. Sci. 3, 154–166.
Yurt, A., Balaban, A., Kandemir, S.U., Bereket, G., Erk, B., 2004. Mater. Chem. Phys. 85, 420–426.

Please cite this article in press as: Muthukrishnan, P. et al., Stigmasterol extracted from *Ficus hispida* leaves as a green inhibitor for the mild steel corrosion in 1 M HCl solution. Arabian Journal of Chemistry (2015), http://dx.doi.org/10.1016/j.arabjc.2015.09.005